



Published in final edited form as:

Dev Neurobiol. 2010 June ; 70(7): 508–522. doi:10.1002/dneu.20791.

Na_v1.6a is required for normal activation of motor circuits normally excited by tactile stimulation

Sean E. Low^{1,*}, Weibin Zhou^{2,*}, Xinling Choong², Louis Saint-Amant², Shawn M. Sprague², Hiromi Hirata², Wilson W. Cui³, Richard I. Hume^{1,2}, and John Y. Kuwada^{1,2,3}

¹Neuroscience Program University of Michigan 830 N. University Ave Ann Arbor, MI 48109-1048, USA

²Department of Molecular, Cellular and Developmental Biology University of Michigan 830 N. University Ave Ann Arbor, MI 48109-1048, USA

³Cell and Molecular Biology Program University of Michigan 830 N. University Ave Ann Arbor, MI 48109-1048, USA

Abstract

A screen for zebrafish motor mutants identified two non-complementing alleles of a recessive mutation that were named *non-active* (*nav^{mi89}* and *nav^{mi130}*). *nav* embryos displayed diminished spontaneous and touch-evoked escape behaviors during the first three days of development. Genetic mapping identified the gene encoding Na_v1.6a (*scn8aa*) as a potential candidate for *nav*. Subsequent cloning of *scn8aa* from the two alleles of *nav* uncovered two missense mutations in Na_v1.6a that eliminated channel activity when assayed heterologously. Furthermore the injection of RNA encoding wild type *scn8aa* rescued the *nav* mutant phenotype indicating that *scn8aa* was the causative gene of *nav*.

In vivo electrophysiological analysis of the touch-evoked escape circuit indicated that voltage-dependent inward current was decreased in mechanosensory neurons in mutants, but they were able to fire action potentials. Furthermore tactile stimulation of mutants activated some neurons downstream of mechanosensory neurons but failed to activate the swim locomotor circuit in accord with the behavioral response of initial escape contractions but no swimming. Thus mutant mechanosensory neurons appeared to respond to tactile stimulation but failed to initiate swimming. Interestingly fictive swimming could be initiated pharmacologically suggesting that a swim circuit was present in mutants. These results suggested that Na_v1.6a was required for touch-induced activation of the swim locomotor network.

Keywords

zebrafish; Na_v1.6; *scn8a*; motor behaviors

Introduction

How the activity of genes, and the proteins they encode, contribute to behavior is a central question in neurobiology. To address this question forward genetic screens (Granato et al.

kuwada@umich.edu tel: 734-936-0495 fax: 734-647-0884.

* contributed equally to this study

Present address of H. Hirata: Division of Biological Science, Nagoya University, Nagoya, Japan; S. Low and L. Saint-Amant, Département de Pathologie et Biologie Cellulaire, Université de Montréal; W. Zhou: Life Science Institute, University of Michigan; W. Cui: UCSF School of Medicine.

1996; Baier 2000) have recently been coupled with *in vivo* electrophysiological recordings in zebrafish (Drapeau et al. 1999; Buss and Drapeau 2000). This combined approach has aided in the identification of several genes important for the formation and function of the networks that underlie zebrafish behaviors, in particular motor behaviors (Ono et al. 2002; Ono et al. 2004; Hirata et al. 2004; Cui et al. 2004; Cui et al. 2005; Hirata et al. 2005; Zhou et al. 2006; Hirata et al. 2007).

Within the first two days of development zebrafish embryos perform three highly stereotyped motor behaviors (Saint-Amant and Drapeau 1998). Beginning at ~17 hours post-fertilization (hpf) embryos exhibit spontaneous slow coiling of the trunk and tail. Spontaneous coiling is intrinsic to the spinal cord as it persists following spinalization. Later at ~21 hpf embryos begin to respond to touch with fast and vigorous escape contractions. Lastly at ~28 hpf tactile stimulation evokes escape contractions followed by swimming. Spinalized embryos respond to tactile stimuli with an initial contraction, but subsequent contractions were dramatically reduced and no swimming occurred (Downes and Granato, 2006). By contrast, when embryos were transected between the midbrain and hindbrain, the trunk and tail displayed normal, alternating contractions indistinguishable from those of intact embryos and normal swimming (Saint-Amant and Drapeau, 1998). Thus, the intact hindbrain and spinal cord appear to be necessary and sufficient for the complete touch-evoked escape response and swimming, but the spinal cord may be sufficient for the initial contraction.

As previous mutagenesis screens failed to reach saturation we undertook a forward genetic screen to identify additional behavioral mutants. From this screen two alleles of a mutation named *non-active* (*nav*) were identified. *nav* mutants displayed deficient spontaneous coiling and diminished touch-evoked behaviors. Subsequent cloning and rescue experiments demonstrated that the gene encoding $\text{Na}_v1.6\text{a}$ on chromosome 23 was the causative gene in *nav*. *In vivo* electrophysiological analysis of the escape circuit in *nav* mutants revealed that tactile stimuli activated neurons downstream of mechanosensitive neurons suggesting that mechanosensory neurons were activated, but failed to activate the locomotor network capable of generating swimming. However, swimming could be initiated pharmacologically suggesting that a swimming locomotor network was present in mutants. Thus $\text{Na}_v1.6\text{a}$ was required for touch-induced activation of the swim locomotor network.

Methods

Materials

Unless otherwise noted, reagents were obtained from Sigma Chemical (St. Louis, MO). Tetrodotoxin (TTX) and Riluzole were diluted to the indicated concentrations from stock solutions of 1mM and 100mM, respectively.

Animals

Zebrafish were bred and maintained according to approved guidelines set forth by the University Committee on Use and Care of Animals, University of Michigan. The two alleles of *non-active* (*nav*) *nav^{mi89}* and *nav^{mi130}* were isolated in a mutagenesis screen conducted at the University of Michigan using procedures previously reported (Haffter and Nusslein-Volhard 1996). Prior to an experiment, zebrafish were dechorionated with pronase and developmentally staged as described previously (Kimmel et al. 1995).

Behavioral analysis

Embryos obtained from crosses of *nav* heterozygous carriers were raised at 28.5 °C. Spontaneous coiling was examined in dechorionated embryos at 21-22 h postfertilization

(hpf) for 90 sec each. The amplitude of a coil was measured as the angle that the caudal tip of the tail rotated starting from the longitudinal axis of the embryo. For example when the tip of the tail touched the head the angle of rotation was 180°. The genotype of the embryos was subsequently determined by their response to touch. Touch-evoked behaviors were elicited by touching the tail with a fine tungsten wire (125 µm), or with the tips of a pair of No. 5 forceps. Motor behaviors were recorded by video microscopy using a Panasonic CCD camera (wv-BP330) attached to a Leica dissection microscope at 16 to 32 X magnification. Images were captured (30 Hz) with a Scion LG-3 video card on a Macintosh G4 computer. The images and videos were analyzed offline with the Scion Image software and processed with ImageJ.

Mapping and cloning of *scn8aa*

A mapping family for each allele was established by crossing a *nav^{mi89}* or *nav^{mi130}* female carrier (Michigan local strain) with a wild type WIK male (Zebrafish Resource Center, Eugene, Oregon). One female and one male *nav* carrier were identified for each mapping family and used throughout the mapping process. Bulk segregate analysis (Postlethwait et al. 1994) was conducted according to the Zon lab protocol (<http://zfrhmaps.tch.harvard.edu>) using 20 wild type sibling and 20 mutant embryos. Thereafter 8 wild type siblings and 88 mutant embryos were subjected to intermediate resolution mapping using linked microsatellite (SSLP) markers identified from the bulk segregate analysis. For higher resolution mapping 900 mutants were tested for the linked microsatellite marker Z4421 (<http://zfin.org>).

The *scn8aa* gene was physically mapped to the LN54 radiation hybrid panel by PCR (Hukriede et al. 1999). Primers were designed against the genomic contig Zv4_scaffold 1916 (http://www.ensembl.org/Danio_reio/): forward primer 5'-AAGCCGCCACCTAAGCCAGAC-3'; reverse primer 5'-TGTTGCCACCATGCCAGGAG-3'. To clone *scn8aa* total RNA was isolated from 27-30 hours post-fertilization (hpf) Michigan wild types or homozygous *nav* mutants using Trizol® reagent (Invitrogen, Carlsbad, California, USA). Total cDNA was synthesized using oligo-dT primers and Superscript II reverse transcriptase (Invitrogen, Carlsbad, California, USA) following the manufacturer's protocol (Superscript II manual, version 11-11-203). The coding sequence of *scn8aa* was cloned by PCR from wild type and *nav* mutant cDNA by using 6 pairs of PCR primers designed against the published zebrafish *scn8aa* sequence (NM_131628). PCR products were gel-purified and sequenced, or cloned into the pGEM®-T easy vector (Promega Madison, Wisconsin, USA) prior to sequencing. Sequence analysis was performed using Lasergene software (DNASTar, Madison, Wisconsin, USA).

Expression of *scn8aa* by *Xenopus* oocytes

Wild type *scn8aa* template in pBluescript SK+ was provided by Dr. L.L. Isom (University of Michigan, Ann Arbor). Mutant *scn8aa* templates were obtained by subcloning a fragment encoding the *nav* mutations in place of wild type sequence in the above construct. All mutations were confirmed by DNA sequencing (University of Michigan DNA Sequencing Core), and are referred to using the one letter code such as M1461K, which represents the substitution of methionine 1461 with a lysine.

Capped RNA encoding wild type or mutant *scn8aa* was synthesized using the mMACHINE® mMACHINE® T3 kit (Ambion, Austin, TX). Defolliculated Stage V-VI *Xenopus* oocytes were injected with 12.5 ng of wild type or mutant RNA diluted in 50 nl of DEPC-ddH₂O using a Nanoinject II system (Drummond Scientific Company, Broomall, PA). In some experiments oocytes were co-injected with 12.5 ng of RNA encoding the zebrafish β1 subunit. Following injection oocytes were maintained in Barth's solution at 17°C for 48-72

hours before electrophysiological recordings. Two-electrode voltage clamp recordings were made with an NPI Electronics (Tamm, Germany) TurboTec 3 amplifier. The recording pipette solution contained 3M KCl, and the oocyte external recording solution was as follows (in mM): 90 NaCl, 1 KCl, 1.7 MgCl₂, and 10 HEPES, pH 7.6 (with NaOH). The oocyte external solution was controlled using a BPS-8 solution switcher (ALA Scientific Instruments, Westbury, NY). Experiments were performed at 22 °C by holding oocytes at -100 mV, followed voltage steps to the indicated membrane potentials. Data acquisition and the switching of solutions were controlled by Clampex8.2 (Molecular Devices, Sunnyvale, California, USA) software using a Digidata 1322A interface (Axon Instruments, Union City, CA). Data analysis was performed using Clampfit 9 (Molecular Devices, Sunnyvale, California, USA), and figures were prepared using Sigma Plot 9.0 (SYSTAT Software Inc, Chicago, IL)

To quantify the amplitude of the persistent current an exponential function was first fit to the decay of the inward currents in response to a membrane depolarization from -100 mV to -30 mV. The percent persistent current was defined as the amplitude of current remaining five time constants after the peak current, divided by the amplitude of the peak current.

Mutant rescue

For mutant rescue RNA encoding wild type *scn8aa* was diluted to a concentration of 100 ng/μl in DEPC-ddH₂O containing 0.1% phenol red. Approximately 1.5 ng of RNA (visual assessment) was injected into each embryo at the 1-4 cell stage using a Picospritzer II (Parker Hannifin, Fairfield, NJ).

Whole-mount in situ hybridization and immunolabeling

In situ hybridization was carried out following standard lab protocols (Li et al. 2004). The anti-sense DIG-labeled probe for zebrafish *scn8aa* was made from the last 1.3kb of coding sequence hydrolyzed to approximately < 500 base pairs for application to embryos. After quenching the color reaction embryos were mounted in 70% glycerol/PBS and imaged with DIC microscopy.

The zn5 antibody (Trevarrow et al. 1990) recognizes the DM-GRASP Ig superfamily protein (Kanki et al. 1994; Fashena and Westerfield 1999) and labels secondary spinal motor neurons in zebrafish (Beattie et al. 1997; Chandrasekhar et al. 1999). Zn5 (1:10 dilution) followed by Alexa488 tagged secondary antibody was applied to whole-mounted larvae at 66 hpf following previously published protocols (see references above). Larvae were mounted in 75% glycerol and imaged with epi-fluorescence on a upright compound microscope.

In vivo electrophysiology

Embryos (48-52 hpf) were prepared for *in vivo* recordings from axial skeletal muscle and motor neurons as previously described (Ribera and Nusslein-Volhard 1998; Drapeau et al. 1999; Buss and Drapeau 2000). In brief embryos were anesthetized in 1X Evans recording solution (in mM): 134 NaCl, 2.9 KCl, 2.1 CaCl₂, 1.2 MgCl₂, 10 glucose, 10 HEPES, pH 7.8, containing 0.02% tricaine. Embryos were then pinned to a 35 mm dish coated with Sylgard® through the notochord using 25 μm tungsten wires. The skin overlying the trunk and tail was first scored with a broken pipette, and then removed with a pair of fine No.5 forceps. The bath solution was continuously exchanged at ~1 ml/min throughout the recording session with 1X Evans for Mauthner cell recordings, 1X Evans containing 2-3 μM d-tubocurarine for muscle recordings, or 15 μM for Rohon-Beard (RB) and motor neuron recordings. The internal recording solution contained (in mM): 116 K-gluconate, 16 KCl, 2 MgCl₂, 10 HEPES, 10 EGTA, at pH 7.2 with 0.1% sulforhodamineB for cell type

identification. Electrodes pulled from Borosilicate glass had resistances of 6-10 M Ω for muscle, 10-14 M Ω for RB and motor neurons when filled with internal recording solution, and ~1 M Ω when filled with external recording solution for Mauthner cell recordings. To expose the spinal cord for motor neuron and Rohon-Beard recordings the bath solution was replaced with recording solution containing 2 mg/ml collagenase Type XI and incubated at room temperature (22 °C) until the axial skeletal muscle started to separate at the somitic boundaries. Thereafter the muscle was peeled away using suction applied to a broken pipette (~50 μ m). Recordings were made with an Axopatch 200B amplifier (Axon Instruments, Union City, CA) low pass filtered at 5 kHz and sampled at 1-10 kHz. Data acquisition using a Digidata 1322A interface was controlled by pClamp 8.2 software. The initial data analysis was done with Clampfit 9.2, and figures were prepared using Sigma Plot 9.0.

Touch-evoked responses were evoked by pressure application of bath solution via a broken pipette (~20 μ m) to the tail region. The pressure and duration of a stimulus was controlled by a Picospritzer II. NMDA-evoked fictive swimming was achieved by perfusing the bath with recording solution containing 100 μ M NMDA.

Results

nav mutants exhibit abnormal touch-evoked behaviors

Two recessive motor mutants were identified from an ENU-induced mutagenesis screen for behavioral mutations. The behavioral phenotype of the two mutants were similar and complementation analysis revealed that the two mutants were allelic, and were collectively named *non-active* (*nav^{mi89}* and *nav^{mi130}*). At 21 h postfertilization (hpf) spontaneous coiling was both lower in frequency and amplitude in *nav* mutants compared with wild type siblings (Fig. 1A-B). During the second and third day of development mutants displayed diminished touch-evoked behaviors. By ~24 hpf when wild type siblings typically responded to tactile stimuli with two or more fast, escape contractions, *nav* mutants most frequently responded with fewer escape contractions that were less vigorous (Fig. 1C-D). Later at ~48 hpf when wild type siblings normally responded to touch with escape contractions followed by swimming, *nav* mutants performed only escape contractions with no swimming (Fig. 1E). Thus *nav* mutants were able to detect tactile stimuli, but responded with diminished escape behaviors. Interestingly *nav* mutants eventually gained the ability to swim in response to touch by ~60 hpf (Fig. 1F), but they did not survive beyond two weeks.

There is a defect in the nervous system of *nav* mutants

To better understand the genesis of the *nav* phenotype touch-evoked activity within the zebrafish escape circuit was examined (Fig. 2A). Sensitivity to touch in zebrafish was conferred by two groups of mechanosensitive neurons: those within the trigeminal ganglia relayed tactile stimuli to the head, whereas Rohon-Beard neurons (RBs) located within the dorsal spinal cord relayed tactile stimuli to the trunk and tail. Both groups of mechanosensitive neurons projected axons into the hindbrain (Metcalf et al. 1990) to activate ~90 pairs of reticulospinal neurons including the Mauthner (M) cell during escape behaviors (Gahtan et al. 2002). The M cell in turn made monosynaptic contacts with several spinal cord neurons including motor neurons (Jontes et al. 2000) to activate skeletal muscles resulting in locomotion.

As a first level of characterization touch-evoked activity was examined in axial skeletal muscles of the trunk. Axial skeletal muscle in zebrafish was comprised of slow and fast twitch fibers, both of which were active during swimming (Buss and Drapeau 2002). Touch resulted in episodes of rhythmic membrane depolarizations that underlie swimming in slow twitch fibers of wild type siblings (n = 5; Fig. 2B) similar to previous reports (Buss and

Drapeau 2002). In contrast short, arrhythmic depolarizations were observed in *nav* slow twitch fibers in response to touch ($n = 5$). The aberrant responses of muscles in *nav* mutants were consistent with touch-evoked escape contractions, but no swimming in *nav* mutants.

The abnormal touch-evoked response of *nav* muscles could be a result of a defect within the nervous system, or a defect in skeletal muscle that disrupts muscle's ability to respond to sustained input from motor neurons. To determine whether the output of the CNS was defective in *nav* mutants, touch-evoked activity in motor neurons was examined. Recordings made from all three primary motor neurons (CaP, MiP and RoP) revealed that touch evoked a prolonged burst of action potentials in wild type embryos ($n = 5$; Fig. 2C) similar to previous reports (Buss and Drapeau 2001). In contrast touch evoked only a short burst of action potentials in primary motor neurons of *nav* mutants ($n = 5$), consistent with the abbreviated response of skeletal muscles. Thus tactile stimuli was not properly converted into a normal motor output by the nervous system of *nav* mutants.

Touch triggers activity by the Mauthner cell within the escape circuit of *nav* mutants

In fish the M cells are reticulospinal interneurons that receive input from mechanosensitive neurons (Zottoli and Faber 1979), and in turn make monosynaptic contacts with motor neurons (Jontes et al. 2000) (Fig 2A). Activity in M cells follows sensory stimulation (Zottoli 1977), precedes the onset of escape contractions (Eaton et al. 1988), and is sufficient to trigger a weaker and less variable escape contraction compared with that initiated by tactile stimulation (Nissanov et al. 1990). Furthermore, ~90 reticulospinal neurons are known to be activated during escape behaviors suggesting that a full-fledge escape response is mediated by the M cell and numerous other reticulospinal interneurons (Gahtan et al. 2002). To examine whether the M cell is activated by tactile stimulation focal, extracellular recordings were used to monitor their spiking activity (Eaton and Farley 1975). Such records reveal that touch evokes spiking by M cells of both wild type siblings ($n = 5$) and *nav* mutants ($n = 5$) at 48-52 hpf (Fig. 2D). Thus sensory information is capable of activating the M cell in mutant embryos to initiate escape responses albeit diminished ones. Since the weaker escape response of *nav* mutants is reminiscent of escape responses induced by direct stimulation of the M cells, it may be possible that many of the other reticulospinal interneurons normally activated by tactile stimulation may fail to do so in *nav* mutants.

RBs in *nav* mutants exhibit reduced sodium currents

Tactile stimuli likely activated mechanosensory neurons in *nav* mutants since the M cell is activated and mutants respond to touch albeit with a diminished response. However it is still possible that the response of mechanosensory neurons although sufficient to activate the M cell in mutants may not be able to activate other reticulospinal interneurons that may normally be activated in a full-fledge escape response. To see if diminished touch-evoked behaviors might be explained by reduced excitability of mechanosensory neurons, RBs were examined by whole-cell voltage and current clamp recordings between 48-52 hpf. In wild type RBs membrane depolarization evoked a rapidly activating-inactivating inward current (3.04 ± 0.16 nA, $n = 12$), followed by a prolonged outward current (Fig. 3A, B). The application of TTX to the bath blocked all the inward current ($n=3$, not shown) consistent with the reported TTX sensitivity of voltage-gated sodium channels expressed by RBs (Pineda et al. 2005). In RBs of *nav* mutants membrane depolarizations also evoked inward currents in all RBs examined. However the average peak inward current in mutant RBs was reduced to approximately 70% of wild type (2.12 ± 0.35 nA, $n = 12$; t-test, $p < 0.05$). The voltage-gated outward currents were comparable between wild type and mutants: the peak I_{out} at $V_{hold} = +80$ mV for wt was 3108 ± 256 pA and for *nav* was 2522 ± 382 pA (t-test, $p = 0.22$). When studied under current clamp conditions, short depolarizing current injections resulted in a single overshooting action potential in wild type ($n=10$) RBs (Fig. 3C), and

prolonged (100 ms) suprathreshold current pulses elicited a single action potential but failed to generate trains of action potentials (not shown). This suggested that RBs are unlikely to respond to tactile stimulation with a train of spikes. Interestingly, current injections into RBs from *nav* mutants (n=8) also elicited a single action potential. These findings demonstrated that although RBs in *nav* mutants exhibited diminished voltage-gated sodium currents, they retained the ability to fire action potentials, and suggested that the properties of neurons postsynaptic to sensory neurons may also be affected in mutants.

Fictive swimming can be generated by *nav* mutants

Analysis of the *nav* touch-evoked escape circuit revealed that mutants detected tactile stimuli, activated the M cell and initiated escape responses at 48 hpf. Yet tactile stimuli failed to initiate swimming in *nav* mutants. This could be due to a defective swimming circuit or a failure to activate the swim circuit. To discern between these two possibilities fictive swimming was driven within the locomotor network by the application of NMDA, which induced fictive swimming that was similar to tactile stimuli in zebrafish (Cui et al. 2004). NMDA (100 μ M) evoked repetitive bouts of fictive swimming in both wild type (n = 5) and mutant (n = 5) embryos (Fig. 4A-B). Thus an operational swimming circuit was present in mutants suggesting that the lack of touch-induced swimming in mutants may be due to deficient activation of the swim circuit in mutant embryos. However the duration and intra-burst frequency but not the period of NMDA induced fictive swimming episodes in *nav* mutants were decreased compared to wild type siblings (Fig. 4C-D). Thus the mutation also affected some parameters of the swim circuit, but the lack of any swimming response to mechanical stimulation in mutants suggested that the swim circuit was not properly activated.

nav phenotype arises from missense mutations in the gene encoding Na_v1.6a (*scn8aa*) that abolish channel activity

Meiotic mapping showed that microsatellite marker z4421 failed to recombine with either allele (0/1140 meioses). Microsatellite marker z4421 was located on chromosome 23 near the *scn8aa* gene that encoded for the voltage-gated sodium channel Na_v1.6a. Since mutations in mouse *scn8a* exhibited a range of movement defects (Meisler et al. 2002) reminiscent of the *nav* phenotype, zebrafish *scn8aa* cDNA was cloned and sequenced from *nav^{mi89}* and *nav^{mi130}* to see if they harbor mutations. Indeed the predicted amino acid sequences of Na_v1.6a from *nav^{mi89}* and *nav^{mi130}* revealed M1461K and L277Q missense mutations, respectively (Fig. 5A). These mutations occurred at highly conserved residues in Na_v1.6, and in the family of voltage-gated sodium channels as a whole.

To examine the functional consequences of these mutations, RNA from wild type or mutant *scn8aa* were expressed in *Xenopus* oocytes and studied under two-electrode voltage-clamp. Whereas wild type *scn8aa* produced voltage-gated sodium currents similar to previous reports for zebrafish Na_v1.6a (Fein et al. 2007), *nav^{mi89}* mutant *scn8aa* RNAs failed to produce currents different from uninjected oocytes (Fig. 5B). Similarly oocytes injected with *nav^{mi130}* RNA generated no currents beyond those found in uninjected oocytes (not shown). To more accurately recapitulate conditions *in vivo* mutant *scn8aa* RNAs were also co-injected with RNA encoding the zebrafish β 1 subunit, which promotes membrane insertion of voltage-gated sodium channels (Isom et al. 1995). Again no voltage-dependent currents different from uninjected oocytes were observed (not shown). Therefore the two missense mutations in *nav^{mi89}* and *nav^{mi130}* both resulted in non-functional Na_v1.6a channels.

To confirm that *scn8aa* was the causative gene in *nav* mutants RNA encoding wild type *scn8aa* was injected into recently fertilized embryos from a cross between two heterozygotes in an attempt to rescue the *nav* phenotype. Injection of wild type RNA

resulted in a reduction in the percent of embryos at 27 hpf that exhibited the mutant phenotype from the predicted Mendelian ratio of 25% to 15.6% (28/180). To see if mutants were indeed rescued these injected embryos were assayed again at 48 hpf when the effect of the injected wild type *scn8aa* RNA might have worn off. In fact at 48 hpf 26.7% (48/180) of the injected embryos displayed the *nav* phenotype. Therefore 20 of the 180 embryos ($\chi^2 < 0.005$, $n = 180$) that exhibited normal touch-evoked escape behaviors at 27 hpf were *nav* mutants, but displayed a wild type phenotype as a result of the injected wild type *scn8aa* RNA. Thus the *nav* phenotype was due to mutations in *scn8aa* that disrupted Nav1.6a.

***scn8aa* is widely expressed in the zebrafish nervous system**

To better understand how the loss of Nav1.6a resulted in diminished touch-evoked responses in *nav* mutants the expression pattern of *scn8aa* was examined at 24 and 48 hpf. Whole-mount *in situ* hybridization demonstrated that *scn8aa* was expressed in many early neurons in the spinal cord and brain at 24 hpf but not in muscles, consistent with previous reports (Pineda et al. 2005; Novak et al. 2006a; Pineda et al. 2006; Chopra et al. 2007; Chen et al. 2008). The size and positions of some of the *scn8aa*-positive neurons suggested that they were likely posterior lateral line ganglion cells, trigeminal neurons and RB neurons (Fig. 6A, B). At 48 hpf *scn8aa* was expressed widely within the CNS and PNS including sensory neurons (Fig. 6C-E). Thus expression of Nav1.6a by mechanosensory neurons and other neurons in the hindbrain and spinal cord was consistent with the observed physiological effects of the loss of Nav1.6a activity on touch-evoked responses.

Interestingly dorsally projecting motor neurons expressed *scn8aa* and development of these motor neurons was defective when Nav1.6a was knocked down (Pineda et al. 2006). By 66 hpf control larvae had developed the dorsal motor branch, but antisense Morpholino injected larvae had not. However, 66 hpf *nav* mutants exhibited dorsal motor branches comparable to that in wildtype sibs (Fig. 6F, G). Dorsal branches labeled with zn5 antibody (see Methods) were examined in segments 5-15 in 9 wild type sibs and 10 *nav* mutants. Dorsal motor branches were found in 91% (181/198) of the hemisegments in wild type sibs and 95% (209/220) of the hemisegments in *nav* mutants. Thus the genetic loss of Nav1.6a activity appears not to be of consequence for the projection of the dorsal motor branch.

***nav* phenotype correlates with a loss of persistent sodium current**

Although voltage-gated sodium channels are best known for contributing to the rising phase of action potentials in muscle and neurons, a few members, including Nav1.6, exhibit a non-inactivating persistent current (I_{NaP}) (Crill 1996; Raman et al. 1997). Interestingly I_{NaP} is essential for normal fictive locomotion in neonatal rodents (Tazerart et al. 2007; Zhong et al. 2007). Since *nav* mutants fail to initiate swimming following tactile stimulation, the role of I_{NaP} for touch-induced swimming was examined. First zebrafish Nav1.6a was examined to see if it exhibits I_{NaP} by coexpressing RNA encoding Nav1.6a and the $\beta 1$ subunit in *Xenopus* oocytes and studying currents under two-electrode voltage clamp. In response to membrane depolarization a pronounced I_{NaP} was observed (Fig. 7A).

Since I_{NaP} in other organisms was sensitive to the drug Riluzole (Urbani and Belluzzi 2000), the action of Riluzole was examined on I_{NaP} exhibited by zebrafish Nav1.6a. Riluzole preferentially blocked I_{NaP} with minimal effects on transient peak current (Fig. 7A, B). As a first step to determine whether a lack of I_{NaP} might be involved in the *nav* phenotype the behavior of embryos exposed to Riluzole was examined. Within several minutes of exposure to 10 μ M Riluzole wild type embryos (48 hpf) responded to touch with escape contractions but no swimming much like *nav* mutants (Fig. 7C). The lack of swimming in 10 μ M Riluzole treated wild type embryos was due to a touch-induced abbreviated, arrhythmic depolarization in muscles similar to that seen in *nav* mutants (Fig. 7D). Further experiments

are needed to clarify these initial findings, but the results raise the possibility that persistent sodium current is important for the transformation of transient tactile stimuli into prolonged motor behaviors in zebrafish.

Discussion

A forward genetic screen in zebrafish uncovered two alleles of a behavioral mutation that was named *non-active* (*nav*). Both alleles of *nav* exhibited diminished spontaneous coiling similar to that described for NaV1.6a morphants (Tsai et al. 2001) and touch-evoked behaviors during the second and third days of development as a result of missense mutations in the gene encoding NaV1.6a (*scn8aa*) which abolished channel activity.

Skeletal muscles and motor neurons in *nav* mutants responded to tactile stimulation, but the response was of shorter duration compared to wild type siblings. This and the fact that *scn8aa* was not expressed by skeletal muscles (Novak et al. 2006b; Tsai et al. 2001) demonstrated that the *nav* behavioral defect was a consequence of abnormal activity within the nervous system. Although zebrafish motor neurons do express *scn8aa* (Novak et al. 2006b; Pineda et al. 2006; Tsai et al. 2001), the expression of *scn8aa* has been detected only in a subset of motor neurons: the ventrally projecting CaP primary motor neuron, and the dorsally projecting secondary motor neurons. As our recordings were made from all three types of primary motor neurons (CaP, MiP and RoP) and they all exhibited similar patterns of abbreviated bursting, a defect upstream of the motor neurons likely existed in *nav* mutants. Additionally the finding that NMDA evoked fictive swimming in *nav* mutants suggested that mutant motor neurons were capable of providing sustained drive to skeletal muscle when they received adequate synaptic stimulation. Thus the lack of swimming in *nav* mutants involves a defect to neurons that were presynaptic to the motor neurons. Consistent with these findings, the development of motor nerves was unaffected by the loss of NaV1.6a activity in *nav* mutants. Previously NaV1.6a morphants were shown to exhibit defective development of the dorsal branch of the spinal motor nerve (Pineda et al. 2006). The reason for the difference between the *nav* and the morphant results is unclear but one possibility is that genetic compensation such as by other NaVs may occur in *nav* mutants.

The finding that RB neurons can generate action potentials in *nav* mutants despite a decrease in voltage-dependent inward current, and that tactile stimulation activated M cells in mutants suggested that RB neurons do respond to tactile stimulation. One possible explanation for the *nav* phenotype might be that RBs may normally respond to tactile stimuli with a train of action potentials, and that the loss of NaV1.6a might lead to reduce the response to a single spike or shorter burst of spikes. The shortened response of RBs in mutants may be sufficient to activate the M cell and the fast escape contraction but not other reticulospinal interneurons that may normally drive the swim circuit. However, prolonged suprathreshold current injection was unable to initiate a train of action potentials in wild type RBs consistent with the possibility that tactile stimuli elicits only a transient response in RBs. Indeed RBs responded to the onset of mechanosensory stimulation with a single action potential and offset of the stimulus with a single action potential in wild type zebrafish embryos (unpublished results). Since intracellular injection of current can elicit spiking in mutant RBs as in wild type RBs, it seems unlikely that the loss of NaV1.6a unduly affects the responsiveness of mechanosensory neurons to tactile stimuli. This suggests that defects in signaling downstream of the sensory neurons account for the lack of swimming following tactile stimulation in mutants. Furthermore the fact that exogenous NMDA elicits fictive swimming in both wild type and *nav* mutants suggests that the swim circuit was intact in mutants but was inadequately activated. Thus NaV1.6a might be required in neurons postsynaptic to the mechanosensory neurons and upstream of the swim circuit that normally provide excitatory drive to the swim circuit. The additional fact that the duration and

intraburst frequency of the bouts of fictive swimming initiated by NMDA were lower in mutants compared with wild type suggested that Nav1.6a was also required by the swim circuit for normal swimming.

Persistent sodium currents are required in some neurons to generate bursts of action potentials and have been implicated in locomotion by mammals (Tazerart et al. 2007; Zhong et al. 2007; Tazerart et al. 2008). Zebrafish Nav1.6a exhibits persistent current that can be selectively eliminated with the drug Riluzole much like mammalian Nav1.6 (Urbani and Belluzzi 2000). Interestingly, acute application of Riluzole to wild type embryos mimicked the aberrant touch-evoked behavior and synaptic drive to skeletal muscle observed in *nav* mutants. These pharmacological results along with the apparent requirement of Nav1.6a in interneurons upstream of the swim pattern generator are consistent with a requirement of a Nav1.6a persistent current in these upstream neurons. However the hypothesis that Nav1.6a persistent current is required by interneurons that normally activate the swim pattern generator awaits a more complete analysis of the membrane properties of these interneurons in wild type and mutant embryos.

Acknowledgments

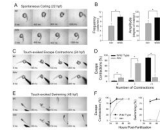
We would like to thank the members of the Kuwada and Hume labs for discussions of the experiments described in this manuscript. We would also like to thank Dr. Lori L. Isom (University of Michigan) for providing wild type *scn8aa*. The work reported here was supported by the National Institute of Neurological Disorders and Stroke (NS054731), and the National Science Foundation (0725976) to J.Y.K. and, National Institute of Neurological Disorders and Strokes to R.I.H., L.S.-A was funded partly by the Fond de Recherche en Santé du Québec, H.H. by a Long-Term Fellowship from the International Human Frontier Science Program and W.W.C. in part by a Center for Organogenesis Training Grant (5-T32-HD007505).

References

- Beattie CE, Hatta K, Halpern ME, Liu H, Eisen JS, Kimmel CB. Temporal separation in the specification of primary and secondary motoneurons in zebrafish. *Dev Biol.* 1997; 187:171–182. [PubMed: 9242415]
- Buss RR, Drapeau P. Activation of embryonic red and white muscle fibers during fictive swimming in the developing zebrafish. *J Neurophysiol.* 2002; 87:1244–1251. [PubMed: 11877498]
- Buss RR, Drapeau P. Physiological properties of zebrafish embryonic red and white muscle fibers during early development. *J Neurophysiology.* 2000; 84:1545–1557.
- Buss RR, Drapeau P. Synaptic drive to motoneurons during fictive swimming in the developing zebrafish. *J Neurophysiol.* 2001; 86:197–210. [PubMed: 11431502]
- Chandrasekhar A, Shcauerte HE, Haffter P, Kuwada JY. The zebrafish *detour* gene is essential for cranial but not spinal motor neuron induction. *Development.* 1999; 126:2727–2737. [PubMed: 10331983]
- Chen YH, Huang FL, Cheng YC, Wu CJ, Yang CN, Tsay HJ. Knockdown of zebrafish Nav1.6 sodium channel impairs embryonic locomotor activities. *J Biomedical Science.* 2008; 15:69–78.
- Chopra SS, Watanabe H, Zhong TP, Roden DM. Molecular cloning and analysis of zebrafish voltage-gated sodium channel beta subunit genes: implications for the evolution of electrical signaling in vertebrates. *BMC Evol Biol.* 2007; 7:113. [PubMed: 17623065]
- Clarke JD, Hayes BP, Hunt SP, Roberts A. Sensory physiology, anatomy and immunohistochemistry of Rohon-Beard neurones in embryos of *Xenopus laevis*. *J Physiol.* 1984; 348:511–525. [PubMed: 6201612]
- Crill WE. Persistent sodium current in mammalian central neurons. *Annual Review Physiol.* 1996; 58:349–362.
- Cui WW, Saint-Amant L, Kuwada JY. *shocked* Gene is required for the function of a premotor network in the zebrafish CNS. *J Neurophysiol.* 2004; 92:2898–2908. [PubMed: 15212431]

- Cui WW, Low SE, Hirata H, Saint-Amant L, Geisler R, Hume RI, Kuwada JY. The zebrafish *shocked* gene encodes a glycine transporter and is essential for the function of early neural circuits in the CNS. *J Neurosci*. 2005; 25:6610–6620. [PubMed: 16014722]
- Drapeau P, Ali DW, Buss RR, Saint-Amant L. In vivo recording from identifiable neurons of the locomotor network in the developing zebrafish. *J Neurosci Methods*. 1999; 88:1–13. [PubMed: 10379574]
- Eaton RC, DiDomenico R, Nissanov J. Flexible body dynamics of the goldfish C-start: implications for reticulospinal command mechanisms. *J Neurosci*. 1988; 8:2758–2768. [PubMed: 3411353]
- Eaton RC, Farley RD. Mauthner neuron field potential in newly hatched larvae of the zebra fish. *J Neurophysiol*. 1975; 38:502–512. [PubMed: 1127453]
- Fashena D, Westerfield M. Secondary motoneuron axons localize DM-GRASP on their fasciculated segments. *J Comp Neurol*. 1999; 406:415–424. [PubMed: 10102505]
- Fein AJ, Meadows LS, Chen C, Slat EA, Isom LL. Cloning and expression of a zebrafish SCN1B ortholog and identification of a species-specific splice variant. *BMC Genomics*. 2007; 8:226. [PubMed: 17623064]
- Gahtan E, Sankrithi N, Campos JB, O'Malley DM. Evidence for a widespread brain stem escape network in larval zebrafish. *J Neurophysiol*. 2002; 87:608–614. [PubMed: 11784774]
- Haffter P, Nusslein-Volhard C. Large scale genetics in a small vertebrate, the zebrafish. *International J Dev Biol*. 1996; 40:221–227.
- Hirata H, Saint-Amant L, Waterbury J, Cui W, Zhou W, Li Q, Goldman D, Granato M, Kuwada JY. *accordion*, a zebrafish behavioral mutant, has a muscle relaxation defect due to a mutation in the ATPase Ca²⁺ pump SERCA1. *Development*. 2004; 131:5457–5468. [PubMed: 15469975]
- Hirata H, Saint-Amant L, Downes GB, Cui WW, Zhou W, Granato M, Kuwada JY. Zebrafish *bandoneon* mutants display behavioral defects due to a mutation in the glycine receptor beta-subunit. *Proc Natl Acad Sci USA*. 2005; 102:8345–8350. [PubMed: 15928085]
- Hirata H, Watanabe T, Hatakeyama J, Sprague SM, Saint-Amant L, Nagashima A, Cui WW, Zhou W, Kuwada JY. Zebrafish *relatively relaxed* mutants have a ryanodine receptor defect, show slow swimming and provide a model of multi-minicore disease. *Development*. 2007; 134:2771–2781. [PubMed: 17596281]
- Hukriede NA, Joly L, Tsang M, Miles J, Tellis P, Epstein JA, Barbazuk WB, Li FN, Paw B, Postlethwait JH, Hudson TJ, Zon LI, McPherson JD, Chevrette M, Dawid IB, Johnson SL, Ekker M. Radiation hybrid mapping of the zebrafish genome. *Proc Natl Acad Sci USA*. 1999; 96:9745–9750. [PubMed: 10449765]
- Isom LL, Scheuer T, Brownstein AB, Ragsdale DS, Murphy BJ, Catterall WA. Functional co-expression of the beta 1 and type IIA alpha subunits of sodium channels in a mammalian cell line. *J Biol Chem*. 1995; 270:3306–3312. [PubMed: 7852416]
- Jontes JD, Buchanan J, Smith SJ. Growth cone and dendrite dynamics in zebrafish embryos: early events in synaptogenesis imaged in vivo. *Nature Neurosci*. 2000; 3:231–237. [PubMed: 10700254]
- Kanki JP, Chang S, Kuwada JY. The molecular cloning and characterization of potential chick DM-GRASP homologs in zebrafish and mouse. *J Neurobiol*. 1994; 25:831–845. [PubMed: 8089660]
- Kimmel CB, Ballard WW, Kimmel SR, Ullmann B, Schilling TF. Stages of embryonic development of the zebrafish. *Dev Dyn*. 1995; 203:253–310. [PubMed: 8589427]
- Korn H, Faber DS. The Mauthner cell half a century later: a neurobiological model for decision-making? *Neuron*. 2005; 47:13–28. [PubMed: 15996545]
- Lefebvre JL, Ono F, Puglielli C, Seidner G, Franzini-Armstrong C, Brehm P, Granato M. Increased neuromuscular activity causes axonal defects and muscular degeneration. *Development*. 2004; 131:2605–2618. [PubMed: 15128655]
- Li Q, Shirabe K, Kuwada JY. Chemokine signaling regulates sensory cell migration in zebrafish. *Dev Biol*. 2004; 269:123–136. [PubMed: 15081362]
- McDearmid JR, Drapeau P. Rhythmic motor activity evoked by NMDA in the spinal zebrafish larva. *J Neurophysiol*. 2006; 95:401–417. [PubMed: 16207779]
- Meisler MH, Kearney JA, Sprunger LK, MacDonald BT, Buchner DA, Escayg A. Mutations of voltage-gated sodium channels in movement disorders and epilepsy. *Novartis Foundation Symposium*. 2002; 241:72–81. discussion 82-76, 226-232. [PubMed: 11771652]

- Nissanov J, Eaton RC, DiDomenico R. The motor output of the Mauthner cell, a reticulospinal command neuron. *Brain Res.* 1990; 517:88–98. [PubMed: 2376010]
- Novak AE, Jost MC, Lu Y, Taylor AD, Zakon HH, Ribera AB. Gene duplications and evolution of vertebrate voltage-gated sodium channels. *J Mol Evol.* 2006a; 63:208–221. [PubMed: 16830092]
- Novak AE, Taylor AD, Pineda RH, Lasda EL, Wright MA, Ribera AB. Embryonic and larval expression of zebrafish voltage-gated sodium channel alpha-subunit genes. *Dev Dyn.* 2006b; 235:1962–1973. [PubMed: 16615064]
- Ono F, Mandel G, Brehm P. Acetylcholine receptors direct rapsyn clusters to the neuromuscular synapse in zebrafish. *J Neurosci.* 2004; 24:5475–5481. [PubMed: 15201319]
- Ono F, Shcherbatko A, Higashijima S, Mandel G, Brehm P. The Zebrafish motility mutant twitch once reveals new roles for rapsyn in synaptic function. *J Neurosci.* 2002; 22:6491–6498. [PubMed: 12151528]
- Pineda RH, Heiser RA, Ribera AB. Developmental, molecular, and genetic dissection of INa in vivo in embryonic zebrafish sensory neurons. *J Neurophysiol.* 2005; 93:3582–3593. [PubMed: 15673553]
- Pineda RH, Svoboda KR, Wright MA, Taylor AD, Novak AE, Gamse JT, Eisen JS, Ribera AB. Knockdown of Nav1.6a Na⁺ channels affects zebrafish motoneuron development. *Development.* 2006; 133:3827–3836. [PubMed: 16943272]
- Postlethwait JH, Johnson SL, Midson CN, Talbot WS, Gates M, Ballinger EW, Africa D, Andrews R, Carl T, Eisen JS, et al. A genetic linkage map for the zebrafish. *Science.* 1994; 264:699–703. [PubMed: 8171321]
- Raman IM, Sprunger LK, Meisler MH, Bean BP. Altered subthreshold sodium currents and disrupted firing patterns in Purkinje neurons of Scn8a mutant mice. *Neuron.* 1997; 19:881–891. [PubMed: 9354334]
- Ribera AB, Nusslein-Volhard C. Zebrafish touch-insensitive mutants reveal an essential role for the developmental regulation of sodium current. *J Neurosci.* 1998; 18:9181–9191. [PubMed: 9801358]
- Saint-Amant L, Drapeau P. Time course of the development of motor behaviors in the zebrafish embryo. *J Neurobiol.* 1998; 37:622–632. [PubMed: 9858263]
- Tazerart S, Viemari JC, Darbon P, Vinay L, Brocard F. Contribution of persistent sodium current to locomotor pattern generation in neonatal rats. *J Neurophysiol.* 2007; 98:613–628. [PubMed: 17567773]
- Tsai CW, Tseng JJ, Lin SC, Chang CY, Wu JL, Horng JF, Tsay HJ. Primary structure and developmental expression of zebrafish sodium channel Na(v)1.6 during neurogenesis. *DNA and Cell Biol.* 2001; 20:249–255. [PubMed: 11410161]
- Urbani A, Belluzzi O. Riluzole inhibits the persistent sodium current in mammalian CNS neurons. *European J Neurosci.* 2000; 12:3567–3574. [PubMed: 11029626]
- Zhong G, Masino MA, Harris-Warrick RM. Persistent sodium currents participate in fictive locomotion generation in neonatal mouse spinal cord. *J Neurosci.* 2007; 27:4507–4518. [PubMed: 17460064]
- Zhou W, Saint-Amant L, Hirata H, Cui WW, Sprague SM, Kuwada JY. Non-sense mutations in the dihydropyridine receptor beta1 gene, CACNB1, paralyze zebrafish *relaxed* mutants. *Cell Calcium.* 2006; 39:227–236. [PubMed: 16368137]
- Zottoli SJ. Correlation of the startle reflex and Mauthner cell auditory responses in unrestrained goldfish. *J Exp Biol.* 1977; 66:243–254. [PubMed: 858992]
- Zottoli SJ, Faber DS. Properties and distribution of anterior VIIIth nerve excitatory inputs to the goldfish Mauthner cell. *Brain Res.* 1979; 174:319–323. [PubMed: 39661]

**Fig. 1.**

nav mutants exhibit abnormal spontaneous coiling amplitude, and diminished touch-evoked behaviors. **(A)** Top: a 22 hpf a wild type sibling exhibiting a single spontaneous coil. Bottom: an aged matched *nav* mutant embryo exhibiting a weaker spontaneous coil when compared to wild type sibs. **(B)** Frequency (left) and amplitude (right) of the spontaneous coils (angle of rotation of the tail) of wild type sib ($n=33$) were greater than that of *nav* mutant ($n=12$) embryos at 21 hpf (t test: $p < 0.01$ for frequency; $p < .05$ for amplitude). **(C)** Top: a 24 hpf wild type sibling touched on the head responds with multiple escape contractions. Bottom: an aged matched *nav* mutant embryo responds with a single contraction. **(D)** Percent of touch-evoked escape contractions consisting of no contractions, one contraction and greater than one contraction in wild type ($n=30$) and *nav* mutant ($n=30$) embryos at 24 hpf. All differences (asterisks) were significantly different (t test: $p < 0.05$). **(E)** Top: a 48 hpf wild type sibling touched on the tail responds with an escape contraction followed by swimming. The embryo appears twice in some frames as the behavior was faster than the video capture rate. Bottom: an aged matched *nav* mutant responds with an escape contraction but no swimming. **(F)** Progression of the *nav* phenotype over the first few days of development compared to wild type. Values represent the average \pm SEM escape response displayed by either wild type or mutant embryo groups ($n = 3$ groups each, 25 embryos each group).

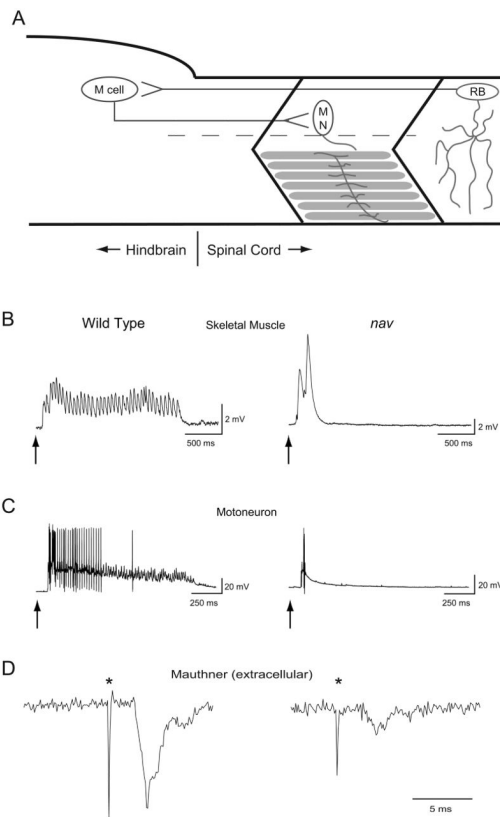


Fig. 2.

Tactile stimulation induces abbreviated bouts of touch-evoked activity in muscle and motor neurons but normal activation of M cells in *nav* mutants. **(A)** A schematic depicting the simplest neural circuit mediating escape contractions. Sensory input from the mechanosensitive Rohon-Beard (RB) neurons activate M cells, which make monosynaptic contacts with motor neurons (MN) that innervate axial skeletal muscle. **(B)** A Prolonged bout of touch-evoked fictive swimming is observed in skeletal muscle of wild type siblings ($n = 5$) while an arrhythmic abbreviated response is recorded in *nav* mutants ($n = 5$). Arrows here and in panel C indicate the approximate time of stimulus. **(C)** Prolonged bouts of touch-evoked bursting in primary motor neurons are observed in wild type sibling ($n = 5$), but not in *nav* mutant ($n = 5$) embryos. **(D)** Touch-evoked M cell spiking recorded extracellularly from wild type sibling (left, $n = 5$) and *nav* mutant (right, $n = 5$) embryos. (*) denotes M cell spiking followed by an electromyogram (EMG). Of note, the amplitude of extracellular activity varies with respect to the location of the recording electrode.

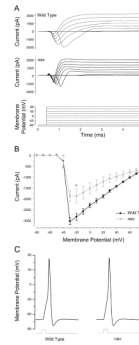


Fig. 3. *nav* RBs exhibit decreased voltage-gated sodium currents, but retain the ability to generate overshooting action potentials. **(A)** Whole-cell current responses recorded in wild type and *nav* mutant RBs (48-52 hpf) following membrane depolarizations. **(B)** Peak inward current plotted as a function of the membrane potential. Values represent the average \pm SEM ($n = 12$ for wild type, and $n = 12$ for mutant). * denotes that difference between wild type and mutant was significant (t- test, $p < 0.05$). **(C)** Action potentials in wild type and *nav* RBs evoked by depolarizing current injections (2 ms) shown below.

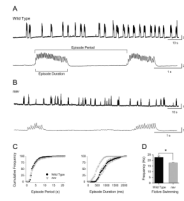


Fig. 4.

Abbreviated fictive swimming can be evoked by NMDA in *nav* mutants (48-52 hpf). **(A)** Top: intracellular voltage recordings showing several minutes of NMDA-evoked fictive swimming from a wild type muscle fiber. Bottom: a faster sweep of two episodes of fictive swimming. **(B)** Top: intracellular voltage recordings showing several minutes of NMDA-evoked fictive swimming from a *nav* mutant fiber. Bottom: a faster sweep of two episodes of fictive swimming. **(C)** Cumulative frequency plots (left) of episode periods from wild type siblings and *nav* mutant embryos ($n = 5$ for each) reveals no difference in how often episodes of fictive swimming are initiated. Cumulative frequency plots (right) of episode durations from wild type siblings and *nav* mutant embryos ($n = 5$ for each) reveals that mutants typically swim for a shorter duration. **(D)** Fictive swimming frequency in *nav* mutants is slower when compared to wild type sibling (* $p < 0.05$).

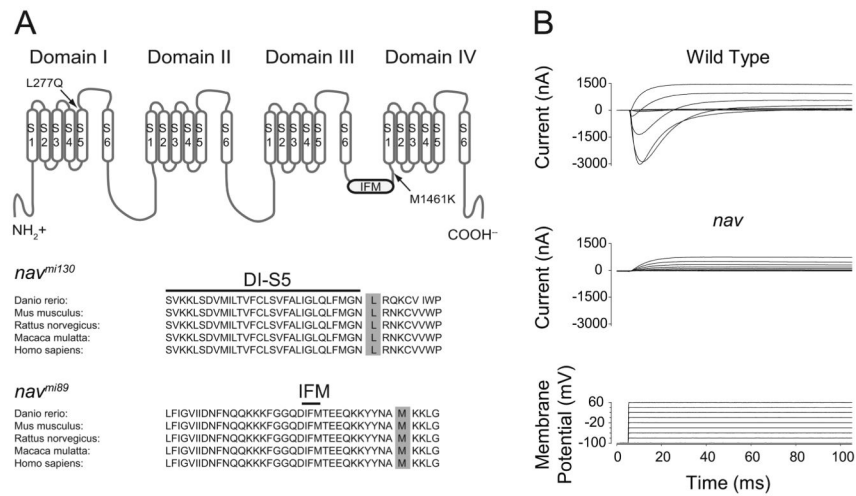


Fig. 5. Missense mutations found in Nav1.6a from *nav*^{mi130} and *nav*^{mi89} abolish channel activity. **(A)** Top: Nav1.6a membrane topology and location of *nav* missense mutations. Bottom: sequence alignment of Nav1.6a from several different species with the conserved leucine 277 and methionine 1461 highlighted in gray. **(B)** Two electrode voltage-clamp recordings made from oocytes injected with either wild type or *nav*^{mi89} RNA. Of note oocytes exhibited variable endogenous outward currents.

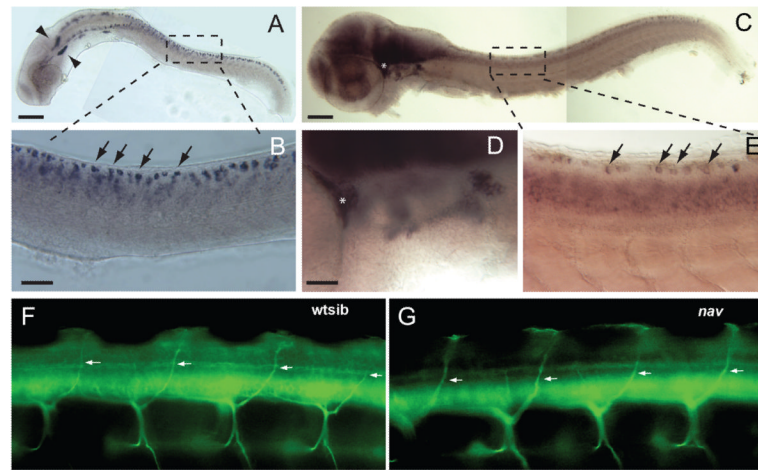


Fig. 6.

scn8aa is widely expressed within the CNS and PNS and motor nerves develop normally in *nav* mutants. (A) Expression of *scn8aa* in a 24 hpf embryo by the posterior lateral line ganglion (arrowheads) and RB neurons. Scale bar, 200 μ m. (B) enlarged image of region indicated in the top panel showing presumptive RB neurons (arrows highlight a few) expressing *scn8aa*. Scale bar, 50 μ m. (C) Expression of *scn8aa* in a 48 hpf embryo is more widespread. Asterisk denotes the trigeminal ganglion which is shown at higher power in (D). Boxed area highlights RBs shown in (E). (D) Enlarged image of region containing the trigeminal ganglion that was denoted by an asterisk in (C). (E) Presumptive RBs (right, arrows highlight a few) expressing *scn8aa*. (F) Sideview of the mid-trunk focused on the dorsal branches of the motor nerves (arrows) in a wild type sibling. Motor nerves were labeled with MAb Zn5 at 66 hpf. (G) Sideview of the mid-trunk showing normal dorsal branches of the motor nerves (arrows) in a *nav* mutant at 66 hpf. Anterior is to the left and dorsal up in both panels.

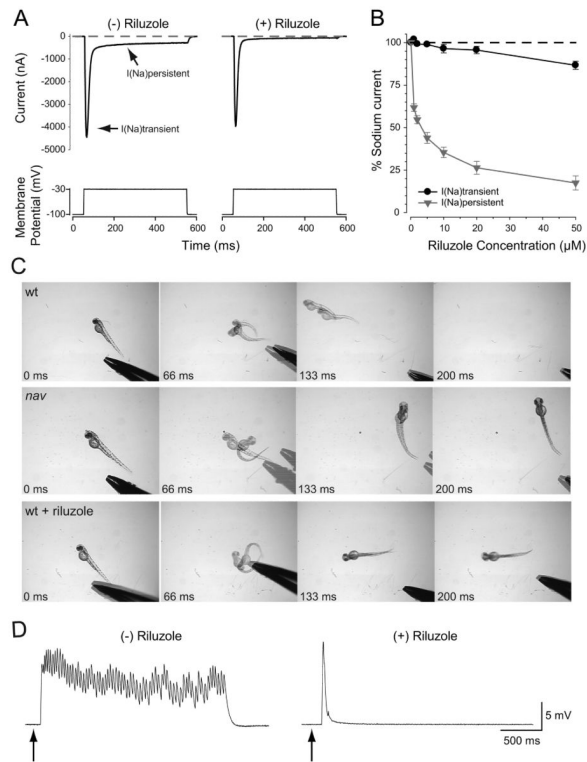


Fig. 7. Riluzole preferentially blocks Na_V1.6a persistent current, and phenocopies the *nav* mutant response to touch in wild type embryos. **(A)** Two electrode voltage clamp recordings from oocytes co-expressing Na_V1.6a and β1 in the absence or presence of Riluzole (50 μM) demonstrating selective blockade of the persistent sodium current. **(B)** Concentration-response relationship of Riluzole effect on persistent and transient sodium currents. Values represent the average ± SEM (*n* = 10). Riluzole (10 μM) mimics the *nav* behavioral response to touch **(C)**, and the abbreviated pattern of touch-evoked synaptic drive to *nav* axial skeletal muscle in wild type embryos (48 hpf) **(D)**.